Interconversion between Three Overstretched DNA Structures

Xinghua Zhang,[†,‡] Yuanyuan Qu,[§,∥] Hu Chen,[‡,⊥] Ioulia Rouzina,[#] Shengli Zhang,[§,⊥] Patrick S. Doyle,*[,†,∇] and Jie Yan*[,†,‡,§,∥]

[†]BioSystems and Micromechanics, Singapore-MIT Alliance for Research and Technology, Singapore 138602, Singapore

[‡]Mechanobiology Institute, National University of Singapore, Singapore 117411, Singapore

[§]Department of Physics, National University of Singapore, Singapore 117551, Singapore

[∥]Centre for Bioimaging Sciences, National University of Singapore, Singapore 117546, Singapore

[⊥]Department of Physics, Xiamen University, Xiamen 361005, China

[#]Department of Biochemistry, Molecular Biology and Biophysics, University of Minnesota, Minneapolis, Minnesota 55455, United States

[⊥]Department of Applied Physics, Xi'an Jiaotong University, Xi'an 710049, China

[∇]Department of Chemical Engineering, Massachusetts Institute of Technology, Cambridge, Massachusetts 02139, United States

ⓢ *Supporting Information*

ABSTRACT: Double-stranded DNA can exist in multiple structures, including three recently identified overstretched structures (peeled ssDNA, DNA bubble, and S-DNA) for torsion-unconstrained DNA under large tension. Here, we report systematic studies of interconversion between these overstretched DNA structures induced by changing NaCl concentration at constant force. At forces above 70 pN where DNA exists in one of the overstretched states, direct interconversions between S-DNA and DNA bubble for the end-closed DNA construct, as well as interconversions between S-DNA and peeled ssDNA for the end-opened DNA construct, were observed to involve stepwise extension changes. Interestingly, compared to other conversions, the conversion from peeled ssDNA to S-DNA has ultraslow kinetics, which can be explained by formation of secondary hairpin structures on a relaxed strand of peeled ssDNA. Our findings provide important insights into the structures of torsion-unconstrained DNA under large force.
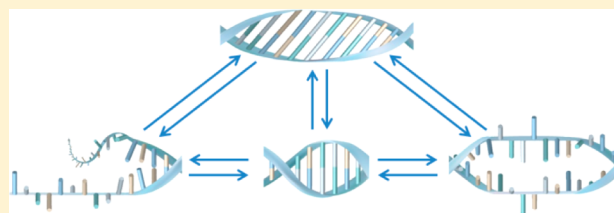
INTRODUCTION

DNA can exist in multiple structures. Single-molecule studies have discovered that when force is increased to ∼65 pN, a structural transition can be induced for torsion-unconstrained DNA, elongating the contour length of B-DNA by ∼1.7 fold during a so-called DNA overstretching transition, as reported in two back-to-back papers in 1996.[1,2] Later studies have revealed the complicated nature of DNA overstretching, suggesting three possible overstretched DNA structures:[3−23] (1) a DNA strand peeling apart from the other at open ends or nicks to produce a single-stranded DNA (ssDNA) under tension while the other strand recoils, namely peeled ssDNA; (2) two DNA stands separating internally to produce two antiparallel ssDNA strands that share tension, namely DNA bubble; and (3) a new form of elongated, base-paired DNA, namely S-DNA.

After 17 years of debate, all of these three hypothesized overstretched DNA structures were recently identified,[24,25] (Figure 1A,B). If DNA has low base-pair stability (favored for AT-rich DNA sequences, low salt concentration, high temperature, etc.), peeled ssDNA is selected for end-opened DNA (note that DNA with open ends is torsion-unconstrained), while DNA bubble is selected for torsion-unconstrained end-closed DNA[19] (both ends are covalently closed, and DNA is linked to surfaces through mono covalent bonds). If DNA has high base-pair stability, S-DNA is selected for both end-opened and end-closed DNA constructs.

The three overstretched DNA structures have distinct force−extension curves: >60 pN, the extensions are ordered $b_{ss} > b_S > b_{bubble}$, where b stands for the extension of a particular DNA structure (Figure 1C). In Figure 1C, the force−extension curve of S-DNA (solid line) was calculated according to the extensible worm-like chain model[26] with parameter determined by our experiments performed at 15 °C and 150 mM NaCl (Figure S2A, Supporting Information). Strictly, the force−extension curve of ssDNA should be dependent on salt concentration of the buffer solution; however, such dependences are negligible at the high forces >50 pN.[12,27] In Figure 1C, the force−extension curve of ssDNA (dashed line) was calculated according to an empirical formula[12] and confirmed by our experiments performed at 15 °C and 1−1000 mM NaCl (Figure S2B, Supporting Information). Finally, the force−extension curve of DNA bubble (dotted line in Figure 1C) was calculated as two noninteracting antiparallel ssDNA strands
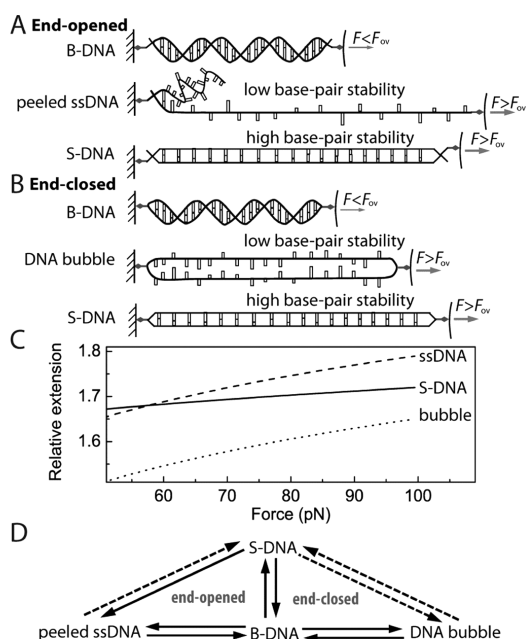
Figure 1. Selection between three overstretched DNA structures. (A) For end-opened DNA, peeled ssDNA is selected if DNA has low base-pair stability, while S-DNA is selected if DNA has high base-pair stability. (B) For end-closed DNA, DNA bubble is selected if DNA has low base-pair stability, while S-DNA is selected if DNA has high base-pair stability. (C) Force—extension curves of the three overstretched DNA structures. Relative extension represents the extension of overstretched DNA relative to the contour length of B-DNA (0.34 nm/bp). (D) Ten possible conversions between four structures of torsion-unconstrained DNA under force. The seven conversions that have been observed are indicated in solid arrows, while the other three conversions that have not been observed are indicated in dashed arrows.

Figure 2. Experimental setup. (A) Four DNA constructs differ in topology and GC percentage: end-closed (1) GC-rich DNA and (2) AT-rich DNA and end-opened (3) GC-rich DNA and (4) AT-rich DNA. (B)Transverse magnetic tweezers with temperature control. (C) A representative time course of DNA extension recorded during changing NaCl concentration from 100 to 5 mM, followed by changing NaCl concentration back to 100 mM at a constant force of 55 pN and 23 °C. The olive arrow indicates the time when new solution containing 5 mM NaCl was passed into the flow cell (defined as time-zero); whereas the cyan arrow indicates the time when new solution containing 100 mM NaCl was passed into the flow cell. Data enclosed in the red rectangle indicate the time course of DNA extension during conversion of B-DNA to peeled ssDNA; while data enclosed in the blue rectangle indicate the time course of DNA extension during conversion from peeled ssDNA back to B-DNA. The experiment was performed for an end-opened AT-rich DNA molecule.

that share force. Please see Force—Extension Curves section in the Supporting Information for more details.

Among the 10 conversions that may occur between the four DNA states (B-DNA, peeled ssDNA, DNA bubble, and S-DNA), six conversions between B-DNA and each of the three overstretched DNA have been excessively studied (Figure 1D). The conversion from S-DNA to peeled ssDNA has also been reported previously.[6,14,17,22] The other three conversions between overstretched DNA structures have not been reported in previous studies. Theoretically, we expect the 10 conversions can be induced by changes in factors that have significant impacts on DNA structural states, such as temperature and salt concentration. In our experiments, we did not use temperature change because it can cause significant instrumentation drift. Instead, we sought to induce the 10 structural conversions by changing of NaCl concentration of the buffer solution and systematically investigated the kinetics of these conversions.

MATERIALS AND METHODS

DNA Constructs. Four DNA constructs were used in this study (Figure 2A): (1) an end-closed[19] GC-rich DNA generated by ligation of a 58% GC DNA segment (amplified from 3198 to 11158 bp of λ DNA) and two short DNA hairpins each carrying a biotin in the middle; (2) an end-closed AT-rich DNA generated similarly, with the inside long DNA segment containing 39% GC contents (amplified from 22374 to 29868 bp of λ DNA); (3) an end-opened GC-rich DNA generated by ligation of a 292 bp 76% GC DNA segment and a 58% GC DNA segment (amplified from 3196 to 10551 bp of λ DNA), with the 3′ end of either DNA strand carrying a biotin; and (4) an
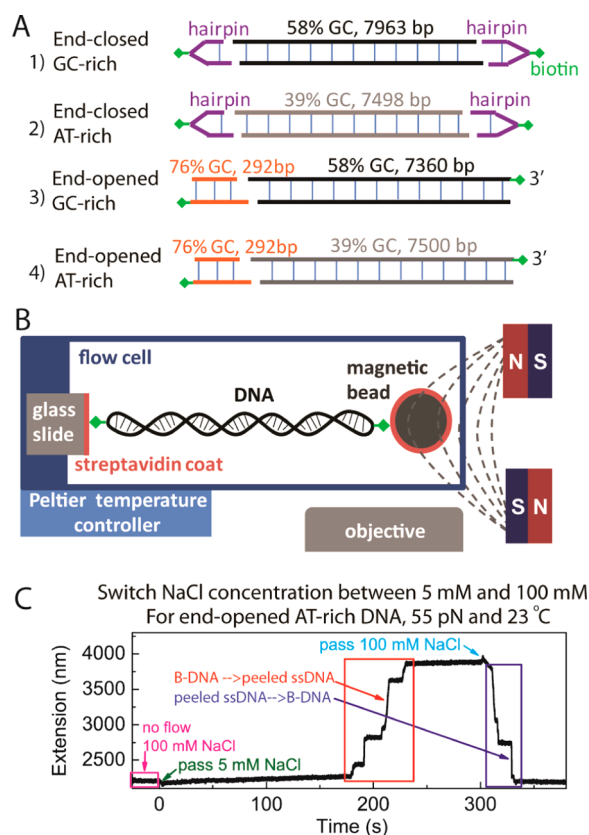
end-opened AT-rich DNA generated similarly, with the inside long DNA segment containing 39% GC contents (amplified from 22374 to 29868 bp of λ DNA). For the two end-closed DNA constructs, peeling from open ends is prohibited topologically, whereas for the two end-opened DNA constructs, peeling is anticipated to start from the less stable open end. See DNA Constructs section in the Supporting Information for detailed protocols.

Transverse Magnetic Tweezers Setup. A transverse magnetic tweezers setup was used to manipulate single DNA molecules (Figure 2B).[28] A DNA molecule with biotin at either terminus was tethered between a streptavidin-coated glass slide and a superparamagnetic bead (Dynabeads M-270 Streptavidin), taking advantage of biotin—streptavidin interactions. A pair of permanent magnets was used to exert constant forces to the tethered DNA molecule. The extension of the DNA molecule was determined as the distance from the bead to the glass slide. The position of the bead was obtained by its centroid, and an offset based on the known force—extension curve of S-DNA was used to find the absolute value of the DNA extension. The stretching force was controlled by the position of the magnets.[21] A

16074

dx.doi.org/10.1021/ja5090805 | *J. Am. Chem. Soc.* 2014, 136, 16073—16080

Peltier chip was used to maintain a low temperature (<23 °C) to increase the lifetime of the biotin–streptavidin bond.[29]

Changing NaCl Concentration in the Flow Cell. Buffer solutions of various NaCl concentrations were diluted from 2.5 M NaCl and 0.5 M Tris-HCl, pH 7.5 with distilled water. A syringe pump (NE-1000, New Era Pump Systems) was used to change the NaCl concentration by passing new solutions into the ∼80 μL flow cell, while a DNA molecule was stretched at a large force, during which the extension of DNA was monitored and recorded (Figure 2C). A constant low flow speed of 8 μL/s was used to avoid generating significant drag force to the bead. In our experiments, the solution exchange procedure is basically a gradual continuous concentration changing process. We note that it took a much longer time to decrease to a target NaCl concentration than to increase the NaCl concentration. For example, during the process of changing NaCl concentration from 100 to 5 mM, after 90% solution is replaced in the flow cell, the actual NaCl concentration in the flow cell (14.5 mM) is still about three times that of the targeted low NaCl concentration. In contrast, during the reverse solution changing process from 5 to 100 mM, after 90% solution is replaced, the actual NaCl concentration in the flow cell (90.5 mM) is very close to the targeted NaCl concentration.

RESULTS

DNA Overstretching Transitions as a Function of NaCl Concentration. To study how the overstretching transition type and transition force (F_{ov}) depend on NaCl concentration for the DNA sequences, we probed the overstretching transition type and the value of F_{ov} by a force-cycling procedure at the onset of the transition at 23 °C, where mostly only one type of transition can occur[21,24] (Figure 3A–C). During the force-cycling procedure, the applied force was cycled between a fixed force (light gray) about 3 pN lower than F_{ov} and a series of increasing higher forces (dark gray). At each of the higher forces, the variance in DNA extension fluctuation was measured for 10 s. Analogous to other phase transitions, the variance in DNA extension increased dramatically at the onset of DNA overstretching transition. If the variance in DNA extension was greater than a threshold of 200 nm² which is much greater than that of B-DNA at >35 pN (<50 nm² for the length of our DNA), we recorded the value of this higher force as a transition force. We determined the value of F_{ov} to be the average of three lowest recorded transition forces in three repeating force-cycling procedures.

Besides having different force–extension curves for different overstretched DNA structures (Figure 1C), the different transitions to the respective overstretched DNA structures are often associated with different kinetics. For large DNA with sufficient sequence heterogeneity, hysteresis always exists during force-induced DNA melting caused by a melting fork movement across sequence-dependent energy barriers.[17,18,20,23,25,30] In contrast, the B-to-S transition has been shown by many laboratories to lack hysteresis.[13,16,19,23] In this study, the overstretching transition type was determined by whether hysteresis exists at the onset of the DNA overstretching transition. We determined the hysteretic transition for the end-closed DNA constructs to be bubbling (Figure 3A), and the hysteretic transition for the end-opened DNA constructs to be peeling (Figure 3C). In contrast, the nonhysteretic transition for both the end-closed and end-opened DNA constructs was the B-to-S transition (Figure 3B).

The onset of bubbling for end-closed DNA (Figure 3A) was marked by a much larger jump in extension than that of the onset of peeling for end-opened DNA (Figure 3C). The larger jump in extension at onset of bubbling was a general trend
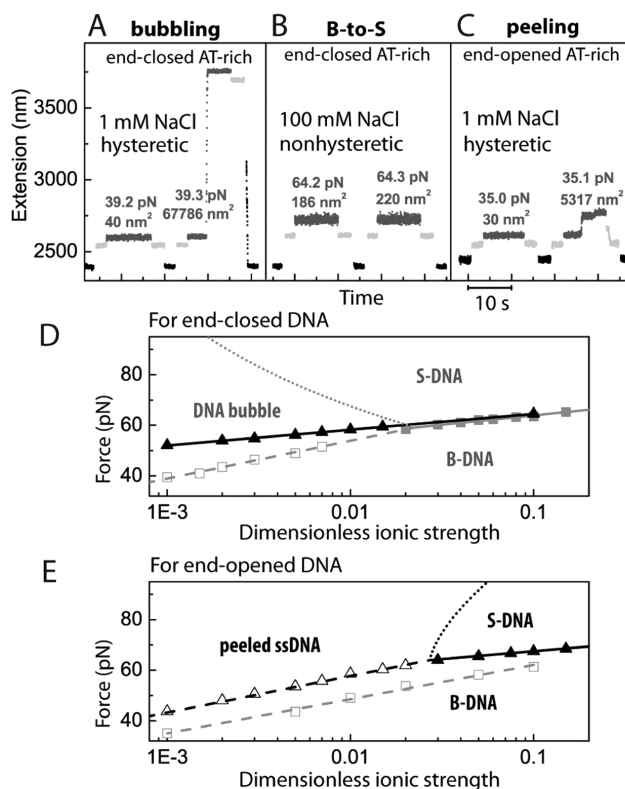

Figure 3. Effects of NaCl concentration to overstretching transitions at 23 °C. (A–C) Representative force-cycling procedure to probe the onset of overstretching transition. During the procedure, the applied force was cycled between a fixed force (light gray) of ∼3 pN lower than overstretching transition force (F_{ov}) and a series of increasing higher forces (dark gray) until the onset of the transition (indicated by sharp increase in DNA extension fluctuation) was observed. Data of two successive of these force cycles are included in the figure, one preceding the transition and one undergoing transition. The value of each higher force and the variance in DNA extension fluctuation are indicated in the figure. A force of 20 pN (black) was used to speed up the reannealing process. (D, E) F_{ov} as a function of dimensionless ionic strength (the molar concentration of NaCl divided by 1 M) for end-closed (D) and end-opened (E) DNA constructs with GC-rich (black triangles) and AT-rich (gray squares) sequences. Each data point represents the average of F_{ov} obtained in more than six experiments from more than three DNA molecules. The standard errors are not plotted since they are smaller than the symbol size (<2 pN). In the nonhysteretic B-to-S transition, F_{ov} is denoted by filled symbols and fitted to a linear function (solid line); whereas in the hysteretic peeling or bubbling transition, F_{ov} is denoted by open symbols and fitted to a linear function (dashed line). The solid and dashed lines each separate two phases of B-DNA and one overstretched DNA structure. Dotted curves indicate the boundary between S-DNA and peeled ssDNA or the boundary between S-DNA and DNA bubble. See Salt Effects section in the Supporting Information for calculation of the dotted slopes.

observed in almost all our experiments, which was likely due to the different activation energy barriers for bubbling and peeling: melting the first base pair in bubbling requires breaking two stacking interactions with the two neighboring base pairs; whereas melting the first base pair in peeling only needs to break one stacking interaction with its neighboring base pair. The larger initial energy cost involved in the bubbling results in a high force to initiate the transition, which could be higher than that needed to break many sequential base pairs during fork movement until it is blocked by a GC-rich island.

For the end-closed DNA constructs (Figure 3D), we found that the AT-rich DNA underwent the nonhysteretic B-to-S transition at >20 mM NaCl (filled gray squares). It underwent the hysteretic bubbling transition at <10 mM NaCl (open gray squares). For comparison, the GC-rich DNA, with higher base-pair stability, underwent the nonhysteric B-to-S transition in the range of 1−100 mM NaCl (filled black triangles). For end-opened DNA constructs (Figure 3E), the GC-rich DNA underwent the nonhysteretic B-to-S transition at >30 mM NaCl (filled black triangles) and the hysteretic peeling transition at <20 mM NaCl (open black triangles). For comparison, AT-rich DNA with a lower base-pair stability underwent the hysteric peeling transition in a range of 1−100 mM NaCl (open gray squares).

Together, these data show the effect of the GC percentage and end-topology to the type of DNA overstretching transitions. In general, the two types of force-induced melting, peeling and bubbling, were preferred for the AT-rich DNA sequences, whereas the B-to-S transition was preferred for the GC-rich DNA constructs.

For DNA sequences with the same GC percentage, the ranges of NaCl concentration where the B-to-S transition or force-induced melting transition (peeling or bubbling) occurred were significantly different between end-closed and end-opened DNA constructs. For AT-rich DNA sequences, the end-closed DNA construct underwent the B-to-S transition at >20 mM NaCl and the bubbling transition at <10 mM NaCl. For comparison, the end-opened DNA construct only underwent the peeling transition in the range of 1−100 mM NaCl.

Note that, since in the DNA bubbles two ssDNA strands share force while in the peeled ssDNA only one ssDNA strand bears the force, for end-opened DNA construct peeling is always favored over bubbling for similar DNA sequences. Consequently, F_{ov} determined in peeling depends on the DNA sequences at the open end. In contrast, as bubbling can start anywhere along DNA, F_{ov} determined in bubbling gives the properties of the weakest DNA sequences inside the DNA.

For any structural transition of DNA between two states i and j under force, the transition force depends on the salt concentration.[8,9,21,31] As pointed out by Rouzina et al.,[8] some insights into the two states can be obtained by studying the transition force as a function of dimensionless ionic strength, $F_{i,j}(I)$ at a constant temperature, where I is the molar concentration of NaCl divided by 1 M. During DNA overstretching transition, an approximately linear relation between $F_{i,j}$ and $\ln(I)$ exists with a slope of $v_{i,j}k_BT/l_B$. Here, $l_B \sim 0.71$ nm is the Bjerrum length and $v_{i,j}=\Delta h_{ij}/\Delta b_{ij}$, where Δh_{ij} is the change in extension per unit charge and Δb_{ij} is the change in extension per base pair projected onto the direction of the force.[8] During DNA overstretching, the value of $v_{i,j}$ can be predicted in three ideal cases, depending on how the two strands in overstretched DNA are associated: $v = 0.5$ if the two strands are under tension with an interstrand distance less than the Debye screening length of several nanometres (case 1); $v \sim 2.4$ if two strands are separate polyelectrolyte chains sharing tension with an interstrand distance much larger than the Debye screening length (case 2); and $0.5 < v < 2.1$ if one strand is under tension while the other recoils (case 3) (see Salt Effects section in the Supporting Information for details of the theory).

In our experiments, all of the three linear fittings for the B-to-S transition give $v_{B,S} = 0.5 \pm 0.1$ (black and gray solid lines in Figure 3D and the black solid line in Figure 3E), consistent with the prediction for case 1; two linear fittings for the peeling transition both give $v_{B,peel} = 1.0 \pm 0.2$ for both GC-rich (the black dashed line in Figure 3E) and AT-rich (the gray dashed line in Figure 3E) DNA sequences, in the range of the predicted value for case 3; the linear fitting for the bubbling transition gives $v_{B,bubble} = 1.2 \pm 0.2$ for AT-rich DNA sequences (the gray dashed line in Figure 3D), indicating that the two strands within the DNA bubble are neither completely together nor separate far away, but somewhere in between. Based on the above three values of $v_{i,j}$ determined by experiments shown in Figure 3D,E, the phase boundary between S-DNA and DNA bubble for AT-rich DNA sequences (the gray dotted line in Figure 3D) and the phase boundary between S-DNA and peeled ssDNA for GC-rich DNA sequences (the black dotted line in Figure 3E) were calculated (see Salt Effects section in the Supporting Information for calculation of these two phase boundaries).

Different DNA States at Different NaCl Concentrations. To induce interconversions between different DNA structures by changing NaCl concentrations at constant force, we need to identify the forces where a DNA construct exists in different states at different NaCl concentrations. Thus, we studied the influence of NaCl concentration on the selection of overstretched DNA structures by a force-scan procedure (Figure 4). This procedure was performed by a force-increase scan until the overstretching transition was completed (filled symbols), followed by a force-decrease scan through the same set of forces (open symbols), during which two force−extension curves, namely the force-increase and the force-decrease curves, were obtained. The structure of overstretched DNA can be judged by comparison of the force-increase and the force-decrease curves.[16,17,21,24,25] During the nonhysteretic B-to-S transition, the two curves overlap each other; whereas during the hysteretic bubbling transition for the end-closed DNA construct or the hysteretic peeling transition for the end-opened DNA construct, such two curves do not overlap. In addition, the DNA bubble is shorter than S-DNA, whereas peeled ssDNA is longer than S-DNA, providing another indicator to distinguish between the three overstretched DNA structures.[12,24]

We found that for the end-closed GC-rich DNA at 23 °C and 1 mM NaCl, the force-increase curve (filled red squares) and the force-decrease curve (open red squares) overlap each other, showing that the DNA molecule underwent the B-to-S transition other than the bubbling transition (Figure 4A). At the higher NaCl concentration of 500 mM (blue triangles), the DNA molecule also underwent the nonhysteretic B-to-S transition but at a higher transition force. Thus, we were able to choose a force of ∼70 pN at which the DNA molecule mainly exists in S-DNA state at 1 mM NaCl while it remains in the B-DNA state at 500 mM NaCl, for the study of the interconversions between B-DNA and S-DNA.

For the end-closed AT-rich DNA (Figure 4B), at 23 °C and 100 mM NaCl, the DNA molecule underwent the non-hysteretic B-to-S transition, indicated by the overlapping force-increase curve (filled blue triangles) and force-decrease curve (open blue triangles). At the lower NaCl concentration of 1 mM with lower base-pair stability, it underwent the hysteretic bubbling transition marked by a nonoverlapping force-increase curve (filled red squares) and force-decrease curve (open red squares). Furthermore, at large forces where the DNA molecule was overstretched at both NaCl concentrations, the DNA bubble at 1 mM NaCl was shorter than the S-DNA at 500 mM
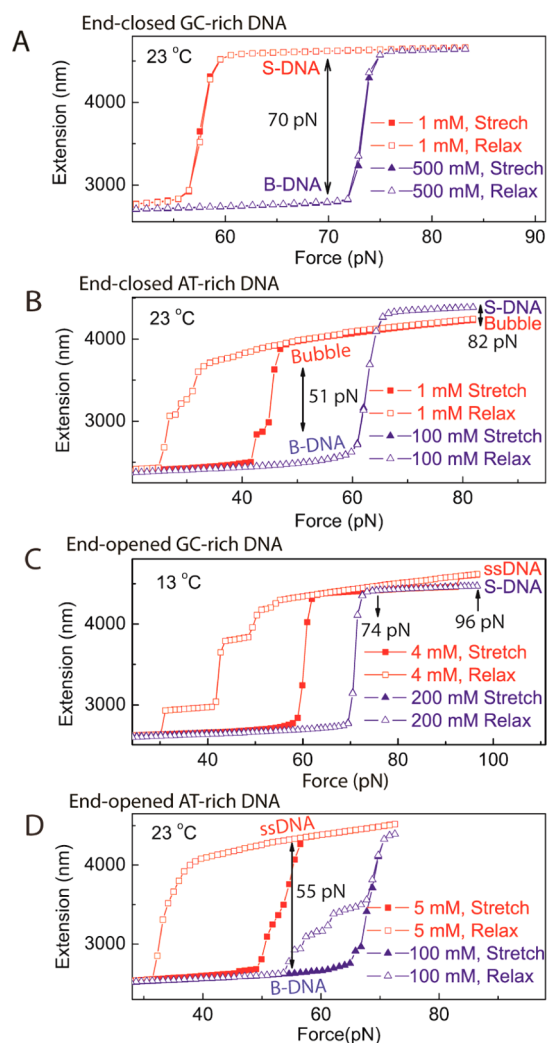
Figure 4. Force−extension curves at a low NaCl (red) and a high NaCl (blue) concentrations for each of the four DNA constructs. At each NaCl concentration for each DNA construct, a force-increase scan (indicated as "Stretch" in the figures, filled symbols) followed by a force-decrease scan (indicated as "Relax" in the figure, open symbols) through the same set of forces were performed. For each data record, the DNA was held for 1 s at each constant force, during which the extension was measured. The black arrows indicate the forces chosen, where the DNA molecule exists in two different states at two different NaCl concentrations.

NaCl. We chose a force of 51 pN at which the DNA molecule mainly exists in the DNA bubble state at 1 mM NaCl, whereas it remains in the B-DNA state at 100 mM NaCl, for the study of the interconversions between B-DNA and DNA bubble. For the same DNA construct (Figure 4B), we also chose another force of 82 pN at which the DNA molecule mainly exists in the DNA bubble state at 1 mM NaCl compared to the S-DNA state at 100 mM NaCl, for the study of interconversions between DNA bubble and S-DNA.

Similarly, the interconversions between S-DNA and peeled ssDNA were studied on end-opened GC-rich DNA (Figure 4C). Two forces of 96 and 74 pN were chosen at which the DNA molecule mainly exists in peeled ssDNA at 4 mM NaCl generated by the hysteretic peeling transition (red squares), whereas it mainly exists in the shorter S-DNA state at 200 mM NaCl generated by the nonhysteretic B-to-S transition (blue triangles). Finally, the interconversions between B-DNA and

peeled ssDNA were studied on end-opened AT-rich DNA at a force of 55 pN (Figure 4D), at which the DNA molecule mainly exists in peeled ssDNA state at 5 mM NaCl (red squares), whereas it remains in the B-DNA states at 100 mM NaCl (blue triangles).

At these chosen constant forces as shown in Figure 4, we next sought to induce the interconversions between two DNA states by switching NaCl concentrations. We monitored the DNA extension while passing the new buffer solution into the flow cell and plotted the time courses of the DNA extension during conversions. For control, before and after the NaCl concentrations were switched and the DNA states were converted, we measured the force−extension curves of the DNA and compared them to the curves measured in Figure 4A−D. In this way, the original and resulting DNA structures were confirmed based on the characteristic force−extension curves of the respective DNA states.

Interconversions between B-DNA and Each of the Three Overstretched DNA Structures. We studied the six conversions between B-DNA and each of the three overstretched DNA structures (S-DNA, peeled ssDNA, and DNA bubble) induced by changing of NaCl concentration at constant forces. For the interconversions between B-DNA and S-DNA induced by switching NaCl concentrations between 1 and 500 mM at 70 pN and 23 °C for the end-closed GC-rich DNA construct, we found that the converting processes are overall gradual and smooth (Figure 5A,B). In contrast, the interconversions between B-DNA and DNA bubble induced by switching NaCl concentrations between 1 and 100 mM at 51 pN and 23 °C for the end-closed AT-rich DNA construct show stepwise dynamics (Figure 5C,D). Similar stepwise dynamics was also observed for interconversions between B-DNA and peeled ssDNA induced by switching NaCl concentrations between 1 and 100 mM at 55 pN and 23 °C for the end-opened AT-rich DNA construct (Figure 5E,F).

These different types of kinetics observed during the various conversions can be attributed to their different nature. For the interconversions between B-DNA and peeled ssDNA (Figure 5E,F), the stepwise dynamics can be explained by the movements of the fork separating the ssDNA and B-DNA cross sequence-dependent energy barriers due to DNA sequence heterogeneity.[17,18,20,23,25,30] The stepwise dynamics of the interconversions between B-DNA and DNA bubble (Figure 5C,D) can also be explained by a similar mechanism, although multiple melting forks may exist since multiple bubbles can be nucleated at locations with weak base-pair stability along the whole DNA sequences. The lack of such stepwise dynamics for the interconversions between B-DNA and S-DNA is consistent with previous studies that suggested much less sequence sensitivity for the B-to-S transition than for DNA melting,[17,18,20,23,25] although a more complex sequence dependence of the B-to-S transition may exist.

We note that the time courses shown in Figure 5 were recorded during passing the new solutions into the flow cell, thus the NaCl concentrations were continuously changing during recording. In such procedure, DNA sequences with weaker base-pair stability may melt before those with stronger base-pair stability during switching from a higher to a lower salt concentration. Similarly, DNA sequences with stronger base-pair stability may reanneal before those with weaker base-pair stability during switching from a lower to a higher salt concentration. However, such effect may not explain the observed stepwise dynamics, as the salt concentration change is
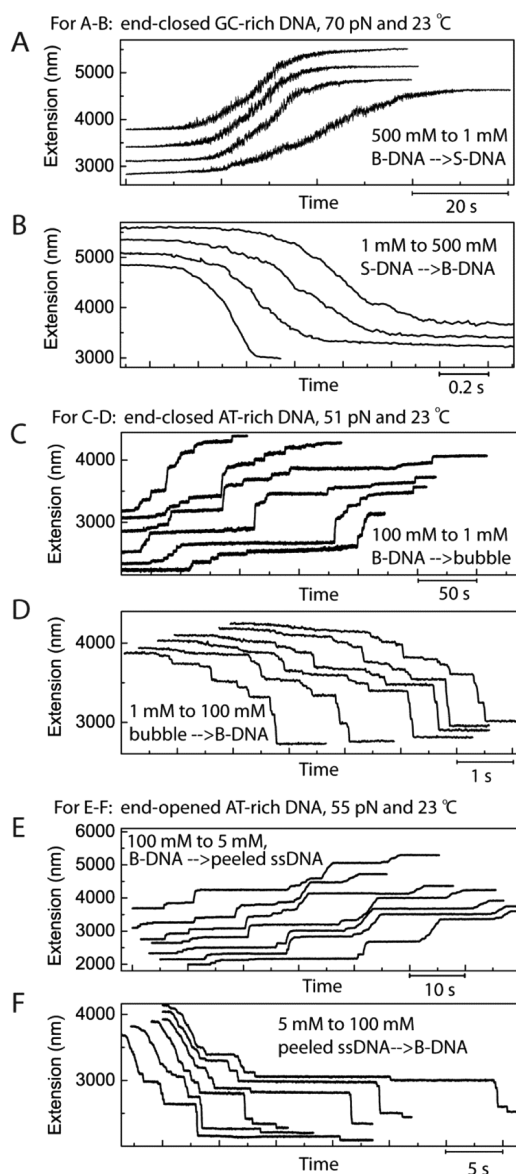
For A-B: end-closed GC-rich DNA, 70 pN and 23 ℃

500 mM to 1 mM
B-DNA --> S-DNA

1 mM to 500 mM
S-DNA --> B-DNA

For C-D: end-closed AT-rich DNA, 51 pN and 23 ℃

100 mM to 1 mM
B-DNA --> bubble

1 mM to 100 mM
bubble --> B-DNA

For E-F: end-opened AT-rich DNA, 55 pN and 23 ℃

100 mM to 5 mM,
B-DNA --> peeled ssDNA

5 mM to 100 mM
peeled ssDNA --> B-DNA

Figure 5. Interconversions between B-DNA and each of the three overstretched DNA structures (S-DNA, peeled ssDNA, and DNA bubble) induced by changing NaCl concentration. In each figure, multiple independent time courses of DNA extension during conversion are shown. For compare, they are shifted in time dimension so that their time when conversion started is similar. Due to the time shift, we used scale bar in the time dimension instead of absolute time. The time courses are also shifted in the extension dimension to avoid overlapping with each other by adding an offset to each of them.

a continuous process. To better demonstrate the stepwise dynamics during interconversions between B-DNA and the two melted DNA structures is an intrinsic nature, we studied these interconversions induced by change in force at constant salt concentrations. Similar stepwise dynamics were also be observed by switching forces at constant NaCl concentrations (see DNA Melting at Constant Salt Concentrations section in Supporting Information). In our study, the conversions induced by increasing of NaCl concentration (overstretched DNA to B-DNA) were faster than the reverse conversion induced by decreasing of NaCl concentration (B-DNA to overstretched DNA). We think this observation is likely due to our solution

exchanging procedure which took much longer time to decrease than to increase NaCl concentration in our procedure (Figure 2C).

Interconversions between S-DNA and DNA Bubble. When we investigated the interconversions between the two overstretched DNA states of the end-closed DNA, S-DNA, and DNA bubble, at forces larger than F_{ov}, we observed a stepwise DNA shortening during decreasing NaCl concentration from 100 to 1 mM at 82 pN and 23 °C (Figure 6A). This finding

End-closed AT-rich DNA, 82 pN and 23 ℃

100 mM to 1 mM
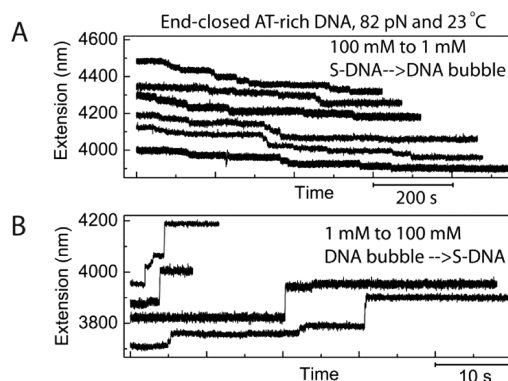S-DNA --> DNA bubble

1 mM to 100 mM
DNA bubble --> S-DNA

Figure 6. Interconversions between S-DNA and DNA bubble induced by changing NaCl concentration at 23 °C and 82 pN for the end-closed AT-rich DNA construct. Time courses obtained from independent DNA molecules were shifted in both the extension and time dimensions for clarity.

indicates the conversion from S-DNA to DNA bubble, as the DNA bubble is shorter than S-DNA at such conditions (Figure 4B). When we reversed the NaCl concentration back to 100 mM from 1 mM, we observed a stepwise DNA elongation back to the original extension of S-DNA (Figure 6B). These results demonstrate that S-DNA and DNA bubble can convert into each other directly by tuning their relative stability though changing NaCl concentration.

Interconversions between S-DNA and Peeled ssDNA. The interconversions between peeled ssDNA and S-DNA were studied similarly at a low temperature of 13 °C, to ensure S-DNA is stable at 200 mM NaCl. When the NaCl concentration was decreasing from 200 mM to 4 mM at 96 pN, we observed stepwise DNA elongation (Figure 7A). As the peeled ssDNA is longer than S-DNA at such conditions (Figure 4C), our results indicate a conversion from S-DNA to peeled ssDNA. Surprisingly, the reverse conversion from peeled ssDNA to S-DNA did not occur even after holding the DNA at 96 pN for 10 min (data now shown). Therefore, we switched to a lower force of 74 pN at which the S-DNA is anticipated to be more stable than at 96 pN.[21] At 74 pN, partial reverse conversion was observed in two of seven independent experiments in our experimental time scale, with an ultraslow kinetics upon switching NaCl concentration back from 4 to 200 mM (Figure 7B). Only a few small DNA shortening steps were observed for seven independent DNA molecules for over 10 min.

We also tried induce the conversion from peeled ssDNA to S-DNA by changing NaCl concentration to 1000 mM at 80 pN. With the increased base-pair stability at 1000 mM NaCl, we anticipated that the reannealing from the peeled ssDNA to S-DNA could be sped up compared to that in 200 mM. In contrast to our anticipation, we did not observe any DNA reannealing steps up to 25 min of DNA holding (Figure 7C). We reason that the difficulty of annealing from peeled ssDNA
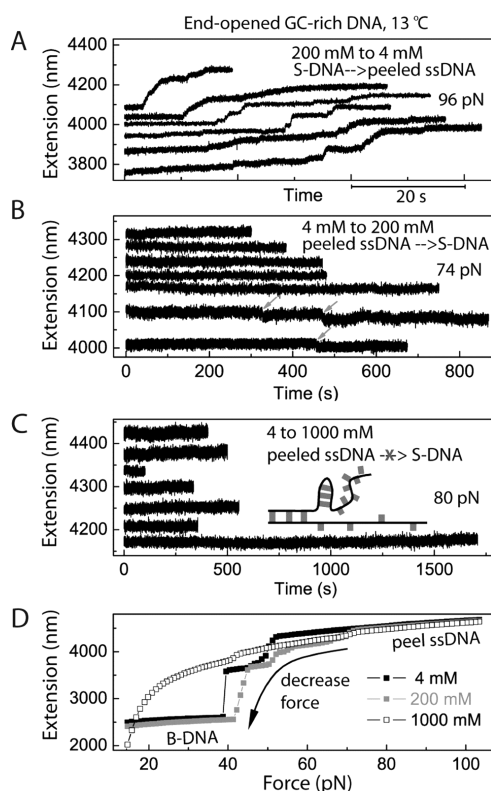
Figure 7. Interconversions between S-DNA and peeled ssDNA induced by changing NaCl concentration for the end-opened GC-rich DNA construct at 13 °C. (A) Time courses of DNA extension recorded during conversion from S-DNA to peeled ssDNA induced by decreasing NaCl concentration from 200 to 4 mM at 96 pN. The data where the conversions were occurring were plotted. Time courses obtained from six independent DNA molecules were shifted in both the extension and time dimensions for clarity. (B) Partial conversion from peeled ssDNA to S-DNA was observed in two of seven independent experiments, induced by increasing NaCl concentration from 4 to 200 mM at 74 pN. The extension-shortening steps are indicated by gray arrows. Time courses obtained from seven independent DNA molecules were shifted in the extension dimension for clarity. The time zero in the figure is the time we began to change solution. (C) Conversion from peeled ssDNA to S-DNA was not observed by increasing NaCl concentration from 4 to 1000 mM in all seven independent experiments. Time courses obtained from seven independent DNA molecules were shifted in the extension dimension for clarity. The time zero in the figure is the time we began to change solution. (D) Force-decrease curves at 4, 200, and 1000 mM NaCl. Reannealing from peeled ssDNA to B-DNA was observed at 4 and 200 mM but not at 1000 mM NaCl.

to S-DNA is due to the formation of secondary hairpin structures on the relaxed ssDNA strand that is not under tension. Such hairpin structures could pose additional energy barriers to annealing (Figure 7C). This mechanism also explains why annealing from peeled ssDNA to S-DNA is even more difficult at 1000 mM NaCl than at 200 mM NaCl, as the secondary structures are expected to be more stable at higher NaCl concentrations.

To further test the mechanism of formation of hairpin structures, we also studied the effects of NaCl concentration on annealing from peeled ssDNA to B-DNA. If such stable secondary structure formed on the relaxed ssDNA, it should also block annealing to B-DNA, particularly at high salt concentration with increased base-pair stability. In this assay, a

peeled ssDNA was produced through peeling of end-opened DNA at 4 mM NaCl. When a force-decrease scan was performed from 103 to 14 pN, during which the DNA extension was recorded at each force for 1 s (Figure 7D), we observed annealing to B-DNA at 38 pN during the force-decrease scan at 4 mM NaCl (filled black squares). For the same DNA molecule, peeled ssDNA was produced again at 4 mM NaCl, and then NaCl concentrations were changed to 200 or 1000 mM at 103 pN. During similar force-decrease scans, annealing to B-DNA was observed at 200 mM NaCl (filled gray squares) but not at 1000 mM NaCl (Figure 7D, open black squares) over our experimental time scale in Figure 7D. Reannealing to B-DNA eventually occurred at 1000 mM NaCl, but after a much longer time scale (see Reannealing of Peeled ssDNA in High Salt Concentration section in Supporting Information).

■ DISCUSSION

In this work, by changing salt concentration at constant temperature and constant force, we have systematically investigated the conversions between four DNA states (B-DNA and three overstretched DNA) for torsion-unconstrained DNA under tension. In total there are 10 possible conversions, as illustrated in Figure 1D. Among them, seven conversions, including six between B-DNA and each of the three overstretched DNA and one from S-DNA to peeled ssDNA, were reported by changing applied force at constant salt concentration in previous studies.[1,2,5,6,9,10,12,14−21,23−25,29−31] Here, we show the seven conversions can also be induced by changing salt concentration at constant force. The remaining three conversions including two between S-DNA and DNA bubbles and one from the peeled ssDNA to S-DNA have been observed for the first time. Importantly, the observed conversions from the two melted DNA states (peeled ssDNA and DNA bubble) to S-DNA provide direct evidence that the S-DNA can be an energetically stable state compared to the two melted DNA states under suitable solution conditions.

The kinetics of the conversions between different DNA states has provided some important insights to the nature of these conversions. Conversions between B-DNA and either of the two melted DNA states are stepwise processes, which are anticipated since DNA melting or annealing involves fork movements across sequence-dependent energy barriers at the boundaries between melted DNA and B-DNA.[17,18,20,23,25,30] Interestingly, conversions between S-DNA and either of the two melted DNA states are also stepwise, suggesting that the fork movements at the boundaries between S-DNA and the melted DNA regions likely also involve crossing sequence-dependent energy barriers. The sequence-dependent base-pair stability of S-DNA remains unclear, which warrants future studies. In contrast to the above melting and annealing conversions, the conversions between B-DNA and S-DNA are smooth processes lacking stepwise extension changes, which is consistent with previous studies.[17,18,20,23,25] However, this observation does not exclude the possibility that the B-to-S transition may also be sequence dependent. In the current and in previous studies, no stepwise dynamics was found during the B-to-S transition. We think the extension fluctuation during B-to-S transition could be too fast to capture by our CCD camera to see possible the transition steps. Therefore, the sequence dependence of the B-to-S transition is still an interesting open question.

Finally, we found that it is difficult to anneal from peeled ssDNA to S-DNA or B-DNA at high salt concentrations where S-DNA or B-DNA is the more stable state compared to peeled ssDNA. This finding is surprising, since such difficulty was not observed in annealing from DNA bubbles to S-DNA or B-DNA. Our explanation of this phenomenon is that in the peeled ssDNA, the relaxed strand that is not under tension can form secondary hairpin structures, thereby causing the kinetic barriers for annealing. Consistent with this explanation, at higher salt concentrations where such hairpins are more stable, we observed even slower annealing processes. This mechanism also explains why annealing from bubbles does not exhibit such difficulties, because the two ssDNA strands in a bubble are both under force that inhibits formation of secondary structure in either of the strands.

■ ASSOCIATED CONTENT

Ⓢ Supporting Information

Details about DNA constructs, force−extension curves, salt effects, reannealing of peeled ssDNA in high salt concentration, and DNA melting at constant salt concentrations. This material is available free of charge via the Internet at http://pubs.acs.org.

■ AUTHOR INFORMATION

Corresponding Authors

phyyj@nus.edu.sg
pdoyle@mit.edu

Notes

The authors declare no competing financial interest.

■ ACKNOWLEDGMENTS

■ REFERENCES

(1) Smith, S. B.; Cui, Y.; Bustamante, C. *Science* **1996**, *271*, 795.
(2) Cluzel, P.; Lebrun, A.; Heller, C.; Lavery, R.; Viovy, J. L.; Chatenay, D.; Caron, F. *Science* **1996**, *271*, 792.
(3) Konrad, M.; Bolonick, J. *J. Am. Chem. Soc.* **1996**, *118*, 10989.
(4) Lebrun, A.; Lavery, R. *Nucleic Acids Res.* **1996**, *24*, 2260.
(5) Leger, J. F.; Romano, G.; Sarkar, A.; Robert, J.; Bourdieu, L.; Chatenay, D.; Marko, J. F. *Phys. Rev. Lett.* **1999**, *83*, 1066.
(6) Rief, M.; Clausen-Schaumann, H.; Gaub, H. E. *Nat. Struct. Biol.* **1999**, *6*, 346.
(7) Rouzina, I.; Bloomfield, V. A. *Biophys. J.* **2001**, *80*, 882.
(8) Rouzina, I.; Bloomfield, V. A. *Biophys. J.* **2001**, *80*, 894.
(9) Wenner, J. R.; Williams, M. C.; Rouzina, I.; Bloomfield, V. A. *Biophys. J.* **2002**, *82*, 3160.
(10) Williams, M. C.; Rouzina, I.; Bloomfield, V. A. *Acc. Chem. Res.* **2002**, *35*, 159.
(11) Bryant, Z.; Stone, M. D.; Gore, J.; Smith, S. B.; Cozzarelli, N. R.; Bustamante, C. *Nature* **2003**, *424*, 338.
(12) Cocco, S.; Yan, J.; Leger, J. F.; Chatenay, D.; Marko, J. F. *Phys. Rev. E* **2004**, *70*, 011910.
(13) Mao, H.; Arias-Gonzalez, J. R.; Smith, S. B.; Tinoco, I., Jr.; Bustamante, C. *Biophys. J.* **2005**, *89*, 1308.
(14) Calderon, C. P.; Chen, W.-H.; Lin, K.-J.; Harris, N. C.; C.-H, K. *J. Phys.: Condens. Matter* **2009**, *21*, 034114.
(15) van Mameren, J.; Gross, P.; Farge, G.; Hooijman, P.; Modesti, M.; Falkenberg, M.; Wuite, G. J.; Peterman, E. J. *Proc. Natl. Acad. Sci. U. S. A.* **2009**, *106*, 18231.
(16) Fu, H.; Chen, H.; Marko, J. F.; Yan, J. *Nucleic Acids Res.* **2010**, *38*, 5594.
(17) Fu, H.; Chen, H.; Zhang, X.; Qu, Y.; Marko, J. F.; Yan, J. *Nucleic Acids Res.* **2011**, *39*, 3473.
(18) Gross, P.; Laurens, N.; Oddershede, L. B.; Bockelmann, U.; Peterman, E. J. G.; Wuite, G. J. L. *Nat. Phys.* **2011**, *7*, 731.
(19) Paik, D. H.; Perkins, T. T. *J. Am. Chem. Soc.* **2011**, *133*, 3219.
(20) Bosaeus, N.; El-Sagheer, Afaf H.; Smith, Steven B.; Åkerman, Björn; Bustamante, Carlos; Nordén, B. *Proc. Natl. Acad. Sci. U. S. A.* **2012**, *109*, 15179.
(21) Zhang, X.; Chen, H.; Fu, H.; Doyle, S. P.; Yan, J. *Proc. Natl. Acad. Sci. U. S. A.* **2012**, *109*, 8103.
(22) Candelli, A.; Hoekstra, T. P.; Farge, G.; Gross, P.; Peterman, E. J.; Wuite, G. J. *Biopolymers* **2013**, *99*, 611.
(23) Bongini, L.; Melli, L.; Lombardi, V.; Bianco, P. *Nucleic Acids Res.* **2014**, *42*, 3436.
(24) Zhang, X.; Chen, H.; Le, S.; Rouzina, I.; Doyle, P. S.; Yan, J. *Proc. Natl. Acad. Sci. U. S. A.* **2013**, *110*, 3865.
(25) King, G. A.; Gross, P.; Bockelmann, U.; Modesti, M.; Wuite, G. J. L.; Peterman, E. J. G. *Proc. Natl. Acad. Sci. U. S. A.* **2013**, *110*, 3859.
(26) Baumann, C. G.; Smith, S. B.; Bloomfield, V. A.; Bustamante, C. *Proc. Natl. Acad. Sci. U. S. A.* **1997**, *94*, 6185.
(27) McIntosh, D. B.; Saleh, O. A. *Macromolecules* **2011**, *44*, 2328.
(28) Yan, J.; Skoko, D.; Marko, J. F. *Phys. Rev. E* **2004**, *70*, 011905.
(29) Beebe, T. P.; Lo, Y. S.; Simons, J. *J. Phys. Chem. B* **2002**, *106*, 9847.
(30) Bosaeus, N.; El-Sagheer, A. H.; Brown, T.; Akerman, B.; Norden, B. *Nucleic Acids Res.* **2014**, *42*, 8083.
(31) Dittmore, A.; Landy, J.; Molzon, A. A.; Saleh, O. A. *J. Am. Chem. Soc.* **2014**, *136*, 5974.